Endo-reduplication in mouse liver after conditional mutation of *ORC2* and combined mutation of *ORC1* and *ORC2*.

Roza K. Przanowska*[1], Yuechuan Chen*[2], Takayuki-Okano Uchida[3], Etsuko Shibata[2], Xiaoxiao Hao[2], Isaac Segura Rueda[2], Kate Jensen[1], Piotr Przanowski[1], Anthony Trimboli[3], Yoshiyuki Shibata[2], Gustavo Leone[3] and Anindya Dutta[1.2, 4]

1: Dept. of Biochemistry and Molecular Genetics, University of Virginia
2: Dept. of Genetics, University of Alabama in Birmingham
3: Cancer Center, University of Wisconsin in Milwaukee.

*Co-first-authors
4: Corresponding author

ABSTRACT

The six subunit Origin Recognition Complex (ORC) is essential for loading MCM2-7 at origins of DNA replication to promote initiation of DNA replication in organisms ranging from *S. cerevisiae* to humans. In rare instances, as in cancer cell-lines in culture with mutations in *ORC1*, *ORC2* or *ORC5*, or in endo-reduplicating mouse hepatocytes *in vivo* without *ORC1*, DNA replication has been observed in the virtual absence of individual ORC subunits. Although *ORC1* is dispensable in the mouse liver for endo-reduplication, because of the homology of ORC1 with CDC6, it could be argued that CDC6 was substituting for ORC1 to restore functional ORC. Here, we have created mice with a conditional deletion of *ORC2*, to demonstrate that mouse embryo fibroblasts require ORC2 for proliferation, but that the mouse hepatocytes can carry out DNA synthesis *in vitro* and endo-reduplicate *in vivo*, despite the deletion of *ORC2*. Combining the conditional mutation of *ORC1* and *ORC2* revealed that the mouse liver can still carry out endo-reduplication despite the deletion of the two genes, both during normal development and after partial hepatectomy. Since endo-reduplication, like normal S phase replication, requires the presence of MCM2-7 on the chromatin, these results suggest that in primary hepatocytes there is a mechanism to load sufficient MCM2-7 to carry out effective DNA replication despite the virtual absence of two subunits of ORC.

INTRODUCTION

DNA replication during normal mitotic cycles or during endo-reduplication is initiated by the six subunit ORC , five of which have AAA+ATPase domains and form a ring shaped complex that binds DNA and bends it (Bell and Stillman, 1992, Neuwald et al., 1999, Dhar et al., 2001a, Clarey et al., 2006, Bleichert et al., 2015). In cooperation with another ATPase, CDC6, and with CDT1, ORC helps load MCM2-7 double hexamers at or near origins of replication(Costa and Diffley, 2022, Stillman, 2022, Hu and Stillman, 2023). To initiate replication (or endo-reduplication), the MCM2-7 hexamer associates with additional proteins to form the functional CMG helicase that is essential for unwinding the double stranded chromosomal DNA, so that the resulting single-stranded DNAs can serve as templates for copying by DNA polymerases. In the lower eukaryotes, various ORC subunits have been consistently found to be essential for DNA replication and cell proliferation (Bell et al., 1993, Foss et al., 1993, Micklem et al., 1993, Loo et al., 1995, Semple et al., 2006). In mammalian cells, knockdown of individual ORC subunits have also been reported to stop cell proliferation (Chou et al., 2021, Prasanth et al., 2004). In humans, mutations in *Orc1*, *Orc4*, *Orc6*, *Cdt1*, and *Cdc6* cause microcephalic primordial dwarfism resembling Meier-Gorlin syndrome (Bicknell et al., 2011b, Bicknell et al., 2011a, Guernsey et al., 2011).

There have, however, been isolated reports that suggest that under unusual circumstances, DNA replication can initiate in eukaryotes in the absence of the full ORC. First hypomorphic mutation made in the *Orc2* gene in HCT116 colon cancer cells decreased ORC2 protein levels by 90% and cells were still viable and could proliferate (Dhar et al., 2001b). Deletion of the *Orc1* gene in Drosophila permitted several rounds of replication in the resulting larvae and pupae (Park and Asano, 2008). A few human cancer cell lines have been created by CRISPR-Cas9 mediated genome engineering where ORC1, ORC2 and ORC5 cannot be detected by regular immunoblots and yet the cell lines survive, proliferate and replicate DNA with the normal complement of origins of replication (Shibata et al., 2016, Shibata and Dutta, 2020). However, the *Orc2* gene is essential for viability and in the *Orc2D* cell line a very minimal level (<0.1% of wild type levels) of a truncated protein can be detected that reacts with anti-ORC2 antibody and co-immunoprecipitates with ORC3(Chou et al., 2021). Given that WT cells have about 150,000

molecules of ORC2, even if this truncated protein is functional ORC2, ~150 molecules of the protein would be expected to load MCM2-7 double hexamers on at least 50,000 origins of replication. This possibility would be consistent with current models of MCM2-7 loading only if ORC was highly catalytic and one ORC hexamer was capable of loading ~667 MCM2-7 hexamers (Costa and Diffley, 2022, Stillman, 2022, Hu and Stillman, 2023).

To address whether the entire ORC holocomplex is essential for DNA replication initiation in primary mammalian cells, we have reported a conditional mutation in the ORC1 gene of mouse (Okano-Uchida et al., 2018). Conditional deletion of *Orc1* (using tissue-specific Cre drivers) revealed that the gene was essential for normal mitotic cell division in intestinal epithelial cells, but that endoreduplication in tissues that are known to become polyploid, like placental trophoblasts and the liver hepatocytes, was unaffected. Because the ORC1 protein is a functional ATPase with sequence homology with CDC6 (Saha et al., 1998, Williams et al., 1997), one possibility that remained was that the mouse CDC6 protein substituted for ORC1 in the ORC holocomplex, producing enough functional ORC. Therefore, we decided to make a conditional mutation in another subunit of ORC, *Orc2*, that does not have the Walker A or B motifs that would make it a functional ATPase and that is not homologous to *Cdc6*. We designed the mutation such that even if an N terminally truncated protein is expressed from a downstream methionine from an alternately spliced mRNA the AAA+ like domain will suffer a significant deletion. This will allow us to test whether the mouse liver survival and endoreduplication after loss of ORC1 is seen even after loss of ORC2. It will also test whether combining the conditional mutations of ORC1 and ORC2 will allow the liver cells to survive and endoreduplicate. If hepatocyte survival and endoreduplication is seen in these mice, then it would be hard to explain this by the substitution of two ORC subunits by the CDC6 protein, and we would gain support for the hypothesis that in rare circumstances even untransformed mammalian cells are capable of loading enough MCM2-7 in the absence of ORC to permit extensive DNA replication.

RESULTS

ORC2 is essential for embryonic development and proliferation of mouse embryo fibroblasts

Mice with Lox P sites inserted flanking exons 6 and 7 of mouse *Orc2* were purchased from Cyagen Biosciences Inc. (**Fig. 1A**). Genotyping with primers F2 and R2 distinguished the loxP marked allele from the WT allele (**Fig. 1B**). In a cross of *Orc2*$^{f/+}$ mice, there was no significant decrease in the yield of *Orc2*$^{f/+}$ or *Orc2*$^{f/f}$ compared to *Orc2*$^{+/+}$ mice (**Fig. 1C**), suggesting that the insertion of the loxP sites in the introns of *Orc2* did not impair the function of ORC2. Recombination between the lox2 sites would delete the coding exons 6 and 7 of *Orc2*, which removes amino acids L111-V150 (**Fig. 1D**). If a transcript is expressed that skips exons 6 and 7, then the resulting protein mutates A110 to V110 and then throws the protein coding sequence out of frame (**Fig 1D**, DORC2), so that the bulk of the 576 amino acid ORC2 protein, including the AAA+ like and WH domains (K230-A576) are not expressed. The AAA+ like domain and the WH domain are key elements for ORC2 assembly into ORC and for ORC function. Even in the remote possibility that a truncated protein is expressed due to alternative splicing and translation initiation from an internal methionine, the next methionine is at M301, so that half of the protein including 70 amino acids of the 239 amino acid AAA+-like domain (K230-G469) would be deleted.

The *Sox2-Cre* allele expresses active Cre during embryonic development. Crossing the *Orc2*$^{f/f}$ mice with *Sox2-Cre* mice resulted in no *Orc2*$^{D/D}$ embryos at E7.5 days onwards suggesting

that embryonic deletion of *Orc2* is lethal (**Table 1**). The near expected number of *Orc2*$^{+/D}$ embryos suggests that hemizygosity of *Orc2* can still support viability.

Mouse embryo fibroblasts (MEF) were obtained from *Orc2*$^{f/f}$ E13.5 day embryos and cultured *in vitro*. 3 days after infection with an Adeno virus expressing Cre, effective recombination between the loxP sites is seen, resulting in a genotype showing that exons 6 and 7 have been deleted in most of the MEF (*Orc2*^{D}) (**Fig. 1E**). Consistent with this, at 5 days after adeno-Cre infection, the ORC2 protein is not detected in the MEF population (**Fig. 1F**). The dilution of the undeleted MEF lysate on the same blot suggests, that if any ORC2 protein is expressed in the MEF after adeno-Cre infection, it is <10% of that in the undeleted MEF. The proliferation rate of the *Orc2*$^{f/f}$ MEF infected with adeno-Cre was highly impaired (**Fig. 1G**). Furthermore, when the MEF were cultured for 15 days, the surviving cells express significant levels of ORC2 (**Fig. 1H**), suggesting that the MEFs that had not undergone the Cre-mediated deletion take over the culture.

Taken together, these results suggest that Cre mediated deletion of exons 6 and 7 of *Orc2* leads to early embryonic lethality and impairs the proliferation of normal diploid MEFs in culture.

Knockout of ORC2 in developing mouse liver

Mice carrying one copy of the Albumin promoter driven Cre gene (*Alb-Cre*) express the Cre recombinase specifically in hepatocytes (Postic et al., 1999). When the *Orc2*$^{f/f}$ mice are crossed with mice carrying *Alb-Cre* (shortened below as *Alb*), the Cre recombinase is expected to promote the recombination mediated deletion of exons 6 and 7 of *Orc2* in the hepatocytes. The *Alb*$^{+/-}$-*Orc2*$^{f/f}$ mice were viable and fertile (**Fig. 2a, 2b**). Crossing such mice yielded the expected numbers of *Alb*$^{+/-}$-*Orc*$^{2f/f}$ mice, though there was a drop in the yield of *Alb*$^{+/+}$-*Orc2*$^{f/f}$ mice. One allele of *Alb-Cre* is sufficient to express enough Cre to carry out homozygous deletion of the *Orc2* allele in the hepatocytes, so that the results suggest that deletion of *Orc2* in the hepatocytes did not impair viability. The partial lethality of the *Alb*$^{+/+}$ (HOM) mice could be due to the toxicity of high dose of Cre recombinase expressed, something that has been noted by other groups (Schmidt et al., 2000, Loonstra et al., 2001, Schmidt-Supprian and Rajewsky, 2007, Naiche and Papaioannou, 2007, Janbandhu et al., 2014). Western blot of liver extract from two mice (M2 and M3) that were *Alb, Orc2*$^{f/f}$ revealed that one of them (M3) expresses less than 20% of the ORC2 protein by comparison of the dilution series of extract from an *Orc2*$^{f/f}$ liver (**Fig. 2c**). Residual ORC2 protein is expected to be expressed mainly in non-hepatocytes and blood cells in the liver. Indeed, when hepatocytes were isolated and genotyped, the hepatocytes from the *Alb, Orc2*$^{f/f}$ livers showed that over 90% of the *Orc2* copies suffered deletion of exons 6 and 7 (**Fig. 4b**, lane 2 compared with lane 3). The body weights of the *Alb, Orc2*$^{f/f}$ mice were smaller than in the *Orc2*$^{f/f}$ animals of both sexes, though the liver size and liver size normalized to body weight was significantly smaller only in the females (**Fig. 2d-f**). There was some elevation of the circulating liver enzymes in the mice where Alb-Cre is expressed to delete the *Orc2* gene, suggesting that there is some impairment of liver function (**Supp. Fig. S1**).

The livers of mice can grow by proliferation (increasing the number of cells) or by hypertrophy of cells (larger cells with endoreduplicated nuclei). Histological examination of the livers revealed that the *Orc2* deletion was accompanied by the presence of fewer (~50% of WT levels), but larger nuclei and cells, and the larger cells had significantly larger nuclei in both males and females (**Fig. 2g-j, Fig. 5e, 0 hr points, Supp. Fig. 3b**). To determine whether the larger nuclei were generated by endoreduplication, we isolated nuclei from hepatocytes and stained them with the DNA staining dye, DRAQ5, followed by flow cytometry (**Fig. 3a**). Both male and

female *Alb, Orc2*$^{f/f}$ livers showed a decrease in 4n DNA content and an increase in 16n DNA content (**Fig. 3b-d**). The expression of Cre would also delete a lox-stop-lox element upstream from EYFP and lead to the expression of EYFP. Indeed, when we gated on EYFP positive cells, the 8n and 16N DNA content increase was much more evident relative to the EYFP negative cells, while the 2N DNA containing nuclei were decreased (**Fig. 3e-h**). Thus *Orc2* deletion promotes endo-reduplication, a result similar to what was noted when *Orc1* was deleted in mouse livers (Okano-Uchida et al., 2018).

DNA replication of *Alb-Cre*$^{+/-}$*-Orc2*$^{f/f}$ hepatocytes *in vitro*.

Primary hepatocytes isolated from 8-10 weeks old mouse liver can replicate their DNA and proliferate for a limited time *in vitro*. We isolated such hepatocytes from *Alb-cre*$^{-/-}$ (WT) and *Alb-cre*$^{+/-}$ livers, both from *Orc2*$^{f/f}$ mice (**Fig. 4a**). Genotyping reveals that over 90% of the cells from the *Alb-cre*$^{+/-}$ livers have successfully deleted *Orc2* exons 6 and 7, while immunoblotting shows that ORC2 protein expression is also significantly decreased in these cells (**Fig. 4b**). EdU labeling *in vitro* for 2 hrs, showed that the EYFP positive cells (where Cre recombinase has been active) can incorporate EdU (**Fig. 4c**), although the total number of nuclei that incorporate EdU is decreased to about 30% of that seen in the ORC2 wild type hepatocytes (**Fig. 4d**).

DNA replication in *Alb-Cre*$^{+/-}$*-Orc2*$^{f/f}$ hepatocytes during liver regeneration *in vivo*.

The liver regenerates to nearly its original weight within 3 days following partial hepatectomy. Such regeneration involves both normal mitotic DNA replication/cell division and endoreduplication accompanied by hypertrophy of the cells. We therefore tested whether deletion of the *Orc2* gene in nearly 90% of the hepatocytes adversely affects liver regeneration after partial hepatectomy in 8-14 weeks old mice (**Fig. 5a**). Although the liver weight after regeneration was smaller than that of WT livers, the liver:body weight ratio was similar in the livers with *Orc2* deletion and *Orc2* WT (**Fig. 5b-d**). The H&E stain of the regenerated liver shows that the liver cells are larger and have larger nuclei in the liver with *Orc2* deletion (**Fig. 5e**). In these experiments, both before and after regeneration, the livers with the Orc2 deletion have ~50% nuclei compared to the wild type livers (**Fig. 5f**). Finally, labeling the livers by injection of EdU in the mice 3-4 hrs before harvesting, shows that the EYFP positive cells (indicating activity of Cre recombinase) were proficient in synthesizing DNA and incorporating EdU (**Fig. 5g, h**). Interestingly, nearly 100% of the hepatocytes were positive for EYFP, suggesting that the Cre recombinase was active in the vast majority of the hepatocytes (**Fig. 5g**). Also, we noted several pairs of EdU positive nuclei (marked by arrows in **Fig. 5g**) whose relative positions suggest that they are sisters born from the same mitosis, suggesting that some EdU positive cells can go through mitosis in the EYFP positive cells. Finally, the nuclei were significantly larger in the Cre active Orc2f/f hepatocytes than in the hepatocytes without Cre, both before and after regeneration (**Fig. 5i**).

Viable mice with endoreduplicated hepatocyte nuclei in *Alb-Orc1*$^{f/f}$ *Orc2*$^{f/f}$ mice.

We have reported that conditional deletion of *Orc1* in developing mouse livers still allowed livers to develop and induced premature endoreduplication, suggesting that significant DNA synthesis can occur in liver cells that are genetically deleted of *Orc1*. We bred the *Orc1*$^{f/f}$ mice with *Orc2*$^{f/f}$ mice to obtain mice where both *Orc1* and *Orc2* are floxed but *Alb-cre* is not present (**Fig. 6a. b**). In this breeding protocol, for unknown reasons there was a decrease in the

percentage of progeny when *Orc2* was floxed in the liver (with or without Orc1 being floxed), but not when just *Orc1* was floxed (**Fig. 6c**). These mice were then bred with *Orc2*$^{f/f}$ *Alb-cre*$^{+/+}$ mice, and the resulting *Orc1*$^{f/+}$, *Orc2*$^{f/f}$, *Alb-cre*$^{+/-}$ mice intercrossed to get *Orc1*$^{f/f}$, *Orc2*$^{f/f}$, *Alb-Cre*$^{+/-}$ mice where the *Orc1* and *Orc2* alleles are conditionally deleted in hepatocytes, and the deletion is accompanied by activation of EYFP expression. H&E staining showed that the double knockout (DKO) female livers have far fewer but larger cells with significantly larger nuclei (**Fig. 6e, Supp. Fig. 2b**) compared to the male livers (**Fig. 6d, 6k**). The female *Alb-Orc1*$^{f/f}$ *Orc2*$^{f/f}$ mice were significantly smaller with smaller livers, decreased liver to body weight ratio and large hepatocyte nuclei (**Fig. 6f, Supp. Fig. 2a, 2b**). We have also observed ~50% lethality of double knock-out female mice within the first month of life, but the remaining 50% survive beyond 4 months of age (**Supp. Fig. 2c**). In contrast, in the male mice, the body and liver weights in the DKO livers were not significantly different from WT livers (**Fig. 6f**, **6h**). By flow cytometry the EYFP positive cells that had seen Cre recombinase activity had distinctly more polyploidization than the EYFP negative cells (**Fig. 6g**). Taken together the results reveal that hepatocytes can synthesize DNA by endoreduplication to produce very large nuclei and very large cells so that the liver size is not hugely decreased, even in the absence of two subunits of ORC. Female mice that have a deletion in two subunits of ORC suffer more morbidity and mortality than male mice.

DNA replication in *Alb-Cre*$^{+/-}$*-Orc1*$^{f/f}$ *Orc2*$^{f/f}$ hepatocytes during liver regeneration *in vivo*.

Finally, partial hepatectomy was performed in the livers of male mice with DKO of *Orc1* and *Orc2*. As can be seen even before partial hepatectomy the body weights were not significantly different from WT mice (**Fig. 6h**). Post regeneration, the liver weights and liver/body weight ratios were not decreased in the DKO mice compared to the WT mice (**Fig. 6i-j**). H&E sections showed that the hepatocyte nuclei were larger and hepatocyte nuclear density lower in the DKO livers both pre-hepatectomy and in the regenerated livers 36 hr post-hepatectomy (**Fig. 6k-m**). EdU labeling for 3-4 hrs before harvesting the livers showed that despite the DKO, the EYFP positive cells showed extensive DNA synthesis (**Fig. 6n**). Even though nearly 100% of the hepatocytes are EYFP positive, the % of nuclei stained with EdU was higher in the DKO regenerating livers (**Fig. 6o**), suggesting that the endoreduplication that accompanies liver regeneration can occur even after deletion of two of the six subunits of ORC.

DISCUSSION

The six subunit ORC is important for recruiting MCM2-7, the core of the replicative DNA helicase and is essential for all forms of DNA replication in eukaryotic cells(Costa and Diffley, 2022, Stillman, 2022, Hu and Stillman, 2023). Yet, it has been possible to select cancer cell-lines that have mutations in *Orc1*, *Orc2* or *Orc5* and do not express detectable levels of the proteins and yet load MCM2-7 to the chromatin and replicate their DNA as they proliferate in culture (Shibata et al., 2016, Shibata and Dutta, 2020). This paradox suggested that there may be an alternative way to load sufficient MCM2-7 on chromatin and support DNA replication, at least in cancer cells in culture. In addition, there have been two instances where *Orc1* has been mutationally removed in *Drosophila* (Park and Asano, 2008) and in mouse hepatocytes or placental trophoblasts (Okano-Uchida et al., 2018), where extensive DNA replication (particularly endo-reduplication in hepatocytes and trophoblasts) has persisted, suggesting that an alternative way of loading MCM2-7 may be available in certain unique cell-cycles that are different from the normal DNA replication that occurs during normal mitotic growth of diploid cells.

Five of the six subunits of ORC (ORC1-5) associate to form ring-shaped structure with interactions between the WH domains and the AAA+ like domains of the five subunits (Bleichert et al., 2015). In mammalian cells only ORC1 and ORC4 have the intact Walker A and B motifs that are necessary for the molecules to act as AAA+ ATPases (Giordano-Coltart et al., 2005). Though this has never been demonstrated experimentally, it is theoretically possible that in the absence of ORC1 in flies or in mouse livers, another related AAA+ ATPase, intimately involved in MCM2-7 loading, CDC6, can substitute for ORC1 to reconstitute a functional 5 subunit ring-shaped ORC-like structure that executes its function (Takeda et al., 2005, Bell, 2017). We therefore wished to test whether removal of a second subunit of ORC, ORC2, that does not have obvious ATPase activity and not much homology to CDC6, would still permit endoreduplication in mouse livers. Given the possibility that a truncated form of ORC2 protein may be expressed in the mutant cells, we took care to design a mutation such that even if a truncated protein was expressed from an internal methionine downstream from the mutation site, such a protein will be missing a significant part of its AAA+ATPase domain. Anyhow, in Western blots we do not see any evidence of such a truncated protein being expressed in the genetically altered MEFs or hepatocytes. In addition, we wondered whether the simultaneous genetic removal of two subunits of ORC, *Orc1* and *Orc2*, would successfully obliterate all forms of DNA replication, including endoreduplication.

Our results show that while *Orc2* is genetically essential for viability of early embryos in utero and mouse embryo fibroblasts *in vitro*, mutational inactivation of *Orc2,* or combined inactivation of *Orc1* and *Orc2*, does not significantly inhibit development of the mouse liver. Adult, viable mice are produced. Albumin expression is activated very early in hepatoblasts in the 7-8 somite stage and the albumin mRNA can be seen in the hepatic primordium emerging from the gut at E9.5 days (Gualdi et al., 1996). ^{3}H-thymidine incorporation can be measured in the liver as late as days 7-14 postnatally (Tilghman and Belayew, 1982), so that many cycles of DNA replication and cell proliferation are expected to occur in hepatoblasts and hepatocytes after the activation of Alb-Cre and subsequent homozygous knockout of *Orc2* (or *Orc1*) in 90% of the hepatocytes.

To estimate the minimal number of cell divisions occurring in the mutant hepatoblasts after the appearance of albumin-driven Cre, we first estimated how many hepatocyte nuclei populate an adult liver. Given that there are 125 million liver cells/gram of tissue (Sohlenius-Sternbeck, 2006), we estimate that there are 162.5 (female) to 218 (male) million nuclei for the 1.3 gram (female) or 1.75 gram (male) livers (all estimates of liver weight and liver nuclear density are from **Fig. 5c, 5f, 6d, S3b, 6f** and **6m**). We next estimated the number of albumin-positive cells early in embryogeneis, from published scRNAseq results that suggest that ~1% of the embryonic cells are of hepatocyte lineage when all embryonic cells are harvested from E9.5-E13.5 embryos (Cao et al., 2019). Given that there are ~200,000 cells in E9.5 embryos (Cao et al., 2019), we expect at most 2,000 albumin positive cells at the stage when albumin mRNA expression is readily detected. Thus, normal development of the liver requires at least 16-17 rounds of diploid cell division from the hepatoblasts/hepatocytes seen in E9.5 embryos to produce the full complement of hepatocyte nuclei in the adult liver (**Table 2,** bottom row). From the weights of the adult livers and the relative densities of the hepatocyte nuclei in the mutant livers, we estimate the total number of hepatocytes in the mutant livers, from which we calculate that the *Orc2-/-* hepatocytes undergo at least 14-16 divisions from the 2000 hepatoblast-stage seen in E9.5 embryo when Cre is induced from the albumin promoter (**Table 2**). Since the *Orc2* deletion is seen in three days (three cell divisions) after Adeno-cre introduction in MEFs (**Fig. 1e**), a conservative estimate is that the deletion is completed in ~5 cell divisions after activation of Albumin-Cre around E9.5.

Thus, in the *Orc2-/-* livers the hepatocytes went through 9-11 rounds of normal duplication after this deletion event to reach the nuclear numbers seen in the *Orc2-/-* livers. Once the *Orc2* gene is deleted, each cell division decreases the ORC2 protein level by half, so that 6 cell divisions would dilute the ORC2 protein to <1.5% of the wild type levels. Therefore, the last 3-5 rounds of diploid cell division occurred with <1.5% of the wild type levels of ORC2. This might suggest that mitotic DNA replication of diploid cells is not completely eliminated in these livers after loss of ORC2. Consistent with this, we see EdU incorporation in EYFP+ hepatocytes, *in vitro*, which, however, could be from a terminal endo-reduplication event. More tantalizing is the presence of *paired* EYFP positive EdU-positive nuclei during the regeneration after partial hepatectomy in 8-14 week old mice. Such paired nuclei are usually seen with daughter nuclei that have just been born from mitosis, suggesting that there were at least a few cells that underwent complete DNA replication and mitosis even though the hepatocytes had activated Cre for over 9-11 weeks through 14-16 rounds of cell division during normal development.

A similar calculation was done for the *Orc1-/-, Orc2-/-* hepatocytes, but separating the female from the male mice, since the nuclear densities were so remarkably different between the sexes (**Table 2**). In the female mice, the albumin positive hepatoblasts seen in E9.5 embryos are calculated to undergo at least 9-11 divisions to produce the adult liver. Thus at least 4-6 rounds can be expected to have occurred after the *Orc* genes were deleted (estimated conservatively as occurring within 5 cell divisions since E9.5). Thus, the last cycles of diploid replication in the female mice could have occurred with 12%-3.3% of the wild type levels of ORC1 and ORC2. In the male mice, the hepatocyte density and liver sizes are higher suggesting that here again, the E9.5 hepatoblasts and their progeny underwent 14-16 rounds of cell division, and that the last 3-5 rounds of diploid cell division occurred with <1.5% of the ORC1 and ORC2 proteins, compared to WT mice.

The male mice appear to be more tolerant of deletion of *Orc2* gene or both *Orc1* and *Orc2* genes, with the livers reaching larger sizes than in the female mice. Plasma testosterone levels reach 50% of adult levels in the first day after birth before declining (to rise again at puberty at 4-5 weeks age), suggesting that enough androgens are present during the proliferative phase of liver development (Bell, 2018). Sex-specific changes in gene expression have been noted to begin in the liver by 3 weeks postnatally (Conforto and Waxman, 2012). Thus, it is possible that androgens directly or indirectly stimulate the division or hypertrophy of hepatocytes to ameliorate the negative effects on liver mass due to the loss of ORC.

In contrast to diploid DNA replication in hepatocytes, we have shown that the livers with a genetic deletion of *Orc2* (or *Orc1* and *Orc2*) undergo endo-reduplication more easily during normal development. Such DNA synthesis is also clearly seen during liver regeneration after partial hepatectomy in the *Orc2-/-* or *Orc1-/-, Orc2-/-* livers. Endoreduplication differs from normal replication in that although the cycles of DNA replication (S phase) are separated by a G1 like phase (G phase) they are not separated by an intervening mitosis and cytokinesis, and is commonly seen during normal development in plants and animals (Shu et al., 2018). However, all evidence suggests that the biochemical mechanism of initiating DNA replication is the same in normal mitotic replication and endoreduplication. For example, cyclin E/cdk kinase activity has to oscillate between low (G phase) and high (S phase) during Drosophila endoreduplication (reviewed in (Lilly and Duronio, 2005)) and the MCM2-7 proteins are associated with the chromatin in G phase and dissociated in S phase as DNA replication occurs (Su and O'Farrell, 1998). Similarly, in the mouse, ablation of cyclin E impairs endoreduplication in megakaryocytes and trophoblasts (Welch, 1992). Overexpression of a factor that helps load MCM2-7 on origins, Cdc6, or genetic ablation of geminin, a factor that inhibits the loading of MCM2-7 on origins,

stimulated endoreduplication in megakaryocytic cells and placental trophoblasts (Bermejo et al., 2002, Gonzalez et al., 2006) (de Renty et al., 2014). Thus, the persistence, and in fact acceleration, of endoreduplication in the mouse livers in the absence of ORC2 and/or ORC1 suggests that there must be an alternate way to recruit sufficient MCM2-7 to the chromatin to support at least the three cycles of endoreduplication required to produce a 16 N nucleus from a 2 N embryonic nucleus during normal development, and to support about two cycles of endoreduplication during liver regeneration.

The acceleration and persistence of endoreduplication even when both *Orc1* and *Orc2* are genetically inactivated, makes it unlikely that a make-shift ORC-like complex is being assembled for loading the MCM2-7 proteins when two out of the five subunits in the ring are missing. Our results are virtually identical to what was observed when we conditionally deleted *Orc1* (Okano-Uchida et al., 2018). There too, normal mitotic DNA replication (in intestinal epithelial cells) was perturbed, but endoreduplication in the liver cells not only persisted but was induced prematurely during development.

There is a possibility that incomplete deletion of *Orc2* or *Orc1* genes in the hepatocytes allows enough liver cells to still carry an *Orc2* or *Orc1* gene to support DNA replication. We think this unlikely, because the *in vitro* DNA replication experiment with hepatocytes shows that although the *Orc2* gene level is decreased to <10% the wild type level, the number of nuclei incorporating EdU are decreased to only 30% the wild type level. Furthermore, in the partial hepatectomy experiment, nearly 100% of the cells are positive for EYFP, suggesting high penetrance in the expression of the Cre recombinase in the hepatocytes, and yet the liver succeeds in endoreduplicating to reach nearly normal liver size. Our antibodies are unable to detect the mouse ORC2 protein by immunostaining, but the immunoblot results on isolated hepatocytes suggest that the protein is significantly decreased when *Alb-cre* is present.

Although the liver size in the *Alb-Cre, Orc2*$^{f/f}$ mice is not significantly decreased relative to body weight, the liver function tests suggest some impairment of liver function. We cannot yet attribute this deficit of liver function to the decrease in number of cells, or to excess endoreduplication, because ORC subunits are also known to be important for epigenetic control of gene expression (Vermeulen et al., 2010). Future experiments will determine whether the liver pathology could be secondary to epigenetic dysregulation of genes important for liver function. The double knockout female mice are sicker, and here some of the explanation may lie in the smaller liver, but here again epigenetic dysregulation in the absence of ORC cannot be ruled out as a potential cause for the morbidity.

In conclusion, while individual ORC subunits are critical for mitotic DNA replication in normal diploid cells in the mouse, some ORC subunits, like ORC1 or ORC2 can be genetically inactivated and still allow DNA replication in endoreduplicating cells like hepatocytes. The mechanism by which MCM2-7 is recruited to origins of replication in the endoreduplicating cells in the absence of two subunits of ORC merits further study.

ACKNOWLEDGEMENT

This work was supported by a grant from the NIH (R01 CA60499 to A.D), Wagner fellowship from the University of Virginia (to R.K.P.), and the F99/K00 NCI Predoctoral to Postdoctoral Fellow Transition Award (F99/K00CA253732 to R.K.P.). This publication was also supported in part by the Medical College of Wisconsin Cancer Center Shared Resources. We thank the following funders for grant support: Advancing a Healthier Wisconsin Endowment (G.L., T.U., A.T.), and the Dr. Glenn R. and Nancy A. Linnerson Endowed Fund (G.L.). We thank the University of Virginia (RRid:SCR_017829) and UAB Flow Cytometry Core Facilities and Research Histology Core

Facilities, that were partially supported by the NCI Grants (P30-CA044579, P30-CA013148), and thank Dr. Ulrike Lorenz from the University of Virginia for the Alb-Cre breeder, and Kody Park for help with genotyping. Figures were created with Biorender.com.

METHODS

Mice

Work involving mice adhered to the guidelines of the Institutional Animal Care and Use Committees (IACUC) at the University of Virginia (protocol number 4198), the University of Alabama at Birmingham (protocol number 22335), the Ohio State University and Medical University of South Carolina. *Orc1* $^{f/f}$ *ROSA26*$^{stop\text{-}EYFP}$ animals were previously reported (Okano-Uchida et al., 2018). *Orc2* $^{f/f}$ mice were generated by Cyagen Biosciences Inc. Exons 6-7 (amino acids L111-V150) was selected as conditional knockout region (cKO). Mouse genomic fragments containing homology arms (HAs) and cKO region were amplified from BAC clone by using high fidelity Taq DNA polymerase and were sequentially assembled into a targeting vector together with recombination sites and selection marker, Neo cassette, flanked by SDA (self-deletion anchor) sites. The linearized vector was electroporated into C57BL/6 ES cells that were subject to G418 selection (200 µg/mL) after 24 hours. 188 G418 resistant clones were picked and amplified in 96-well plates. The PCR screening identified 29 potential targeted clones, from among which 12 were expanded and further characterized by Southern blot analysis. Eleven of the twelve expanded clones were confirmed to be correctly targeted. Targeted ES cell clone N-1F10 was injected into C57BL/6 albino embryos, which were then re-implanted into CD-1 pseudo-pregnant females. Founder animals were identified by their coat color, their germline transmission was confirmed by breeding with C57BL/6 females and subsequent genotyping of the offspring. Three male and five female heterozygous targeted mice were generated from clone N-1F10. Floxed *Orc2* mice were crossed to the *Orc1* $^{f/f}$ *ROSA26*$^{stop\text{-}EYFP}$ animals to generate *Orc2* $^{f/f}$ *ROSA26*$^{stop\text{-}EYFP}$ and *Orc1* $^{f/f}$ *Orc2* $^{f/f}$ *ROSA26*$^{stop\text{-}EYFP}$ strains for usage of EYFP expression as a reporter for Cre recombinase activity and *Orc2* or *Orc1* and *Orc2* deletion. Those were further bred into tissue specific Sox2-Cre (Hayashi et al., 2002) or Alb-Cre (Postic et al., 1999) mice to obtain *Orc2* or *Orc1* and *Orc2* knockout in all cells of the inner cell mass following implantation or in the liver, respectively. All the mice used in this study were maintained in a mixed background (C57BL/6x129x FVB/N).

PCR

Genomic DNA from ear punches was isolated using Quick Extract DNA Extraction Solution (Lucigen., Cat# QE09050). All genotyping PCRs were carried out using MyTaq™ Red Mix (Bioline, Cat# BIO-25043) according to the manufacturer's instructions.

Orc1 genotyping was carried out with primers F1 forward (common to both alleles; 5′-GCTGCTTCAGTGTGGCAATA-3′), R1 reverse (specific for the WT allele; 5′-CTCCAATTGTTCCCCAGCTA-3'), and R2 reverse (specific for deleted allele, 5′-CACCTGTCACTGGACCACAC-3′). The PCR parameters were 95°C for 30 sec, 45× (95°C for 15 sec, 60°C for 20 sec, 72°for 60 sec), 72°C for 5 min. PCR product was run on 2% agarose gel and WT band was detected at 439bp, transgenic band at 310bp, and deleted at 677bp.

Orc2 genotyping was carried out with primers F1 forward (common to both alleles; 5′-GAGGTTGTGGCTGTAATATACGTGATC -3′), and R1 reverse (common to both alleles; 5′-CTGAGCCATCTAACTCCTTCCTAGC -3'), or F2 forward (common to both alleles; 5′-TGGGTAGGTTCATTCCAGTTTAGCC -3′), and R2 reverse (common to both alleles; 5′-ACCTTGGTATTGGACGTCTCTATTC -3'). The PCR parameters were 95°C for 30 sec, 35× (95°C for 15 sec, 55°C for 20 sec, 72°for 60 sec), 72°C for 5 min. To detect constitutive KO allele combination of F1, F2, and R2 was used. PCR product was run on 2% agarose gel and following bands were detected: for F1+R1 – WT at 342bp, and transgenic band at 398bp; for F2+R2 - WT

at 254bp, and transgenic band at 367bp; for F1+F2+R2 - WT at 254bp, transgenic band at 367bp, and deleted at 306bp.
ROSA26 genotyping was carried out with primers F1 forward (common to both alleles; 5′-AAAGTCGCTCTGAGTTGTTAT-3′), R1 reverse (specific for the WT allele; 5′-GGAGCGGGAGAAATGGATAT-3’), and R2 reverse (specific for deleted allele, 5′-GCGAAGAGTTTGTCCTCAACC-3′). The PCR parameters were 95°C for 30 sec, 45× (95°C for 15 sec, 60°C for 20 sec, 72°for 60 sec), 72°C for 5 min. PCR product was run on 2% agarose gel and WT band was detected at 650bp, and transgenic band at 340bp.
Sox2-Cre genotyping was carried out with primers F1 forward (common to both alleles; 5′-ATGCTTCTGTCCGTTTGCCG -3′) and R1 reverse (common to both alleles; 5′-CCTGTTTTGCACGTTCACCG -3’), with Orc1 primers F1 and R1 for an internal control. The PCR parameters were 94°C for 3 min, 38× (94°C for 30 sec, 60°C for 30 sec, 72°C for 40 sec), 72°C for 3 min. PCR product was run on 3% agarose gel and the transgenic band was detected at 875bp with an internal control band at 439bp.
Alb-cre genotyping was carried out with primers Alb-cre-20239-F (specific for the WT allele; 5’-TGCAAACATCACATGCACAC-3’), Alb-cre-olMR5374-F (specific for the transgenic allele; 5’-GAAGCAGAAGCTTAGGAAGATGG-3’) and Alb-cre-20240-R (common to both alleles; 5’-TTGGCCCCTTACCATAACTG-3’). The PCR parameters were 95°C for 30 sec, 35× (95°C for 15 sec, 55°C for 20 sec, 72°for 60 sec), 72°C for 5 min. PCR product was run on 4% agarose gel and WT band was detected at 351bp, and transgenic band at 390bp.
To establish sex of embryos isolated for MEFs, SRY genotyping was carried out with chromosome Y specific forward (5’-TTGTCTAGAGAGCATGGAGGGCCATGT-3’) and reverse primers (5’-CTCCTCTGTGACACTTTAGCCCTCCGA-3’). The PCR parameters were 95°C for 30 sec, 35× (95°C for 15 sec, 55°C for 20 sec, 72°for 60 sec), 72°C for 5 min. PCR product was run on 2% agarose gel and Y-chromosome positive band was detected at 270bp.

MEF isolation and culture
MEFs were isolated from E12.5 *Orc2*$^{+/+}$ or *Orc2*$^{f/f}$ embryos, transformed with SV40 large T antigen and infected with adenovirus Cre-eGFP (#VVC-U of Iowa-1174, University of Iowa). The infected MEFs were cultured for indicated days in DMEM with 10% FBS medium. To measure the cell proliferation, 24 hrs. after the Adenovirus Cre-eGFP transduction, SV40 transformed MEF cells were plated in 96 well plate.
The cell viability was measured every 24 hrs using CellTiter 96® Non-Radioactive Cell Proliferation Assay (Promega, #G4100) according to the manufacturer's instructions. All experiments were conducted in triplicate and absorbance relative to that on day 1 was expressed.

Liver isolation
Control (*Orc2*$^{f/f}$ *ROSA26*$^{stop\text{-}EYFP}$ or *Orc1*$^{f/f}$ *Orc2*$^{f/f}$ *ROSA26*$^{stop\text{-}EYFP}$) and experimental animals (*Alb-Orc2*$^{f/f}$ *ROSA26*$^{stop\text{-}EYFP}$ or *Alb-Orc1*$^{f/f}$ *Orc2*$^{f/f}$ *ROSA26*$^{stop\text{-}EYFP}$) were euthanized using CO_2. Blood was collected was further metabolic studies. Animals were perfused with prewarmed (39°C) Hank's buffered salt solution (HBSS) containing EDTA, $MgCl_2$, and HEPES. The livers were dissected and weighted. Each liver was divided for following experiments: ploidy analysis (right lobe; fresh processing), EYFP flow cytometry (median lobe; fresh processing), immunoblotting and histology (left lobe; half for LN_2 flash freeze and second half into 10% formalin), and genotyping (caudate lobe; LN_2 flash freeze).

Immunoblotting

SV40 transformed MEF with or without adenovirus Cre-eGFP infection were directly lysed in 2x Laemmli Sample Buffer and sonicated. Liver was lysed in modified RIPA buffer (150 mM Sodium Chloride, 50 mM Tris-HCl, pH 7.4, 1 mM EDTA, 1 mM PMSF, 1% Triton X-100, 1% Sodium Deoxycholic Acid, 0.1% SDS) , sonicated, and lysate was clarified by centrifugation. Mouse ORC2 antibody was raised against His tagged full length of ORC2 recombinant protein in Rabbit (Pacific Immunology).

Histology and analysis

All formalin-fixed paraffin-embedded (FFPE) sections and H&E staining were performed by Research Histology Cores at UVA and UAB. Nuclei size was measured using ImageJ 1.50i (Java 1.6.0_24) (56) (Schneider et al., 2012). The number of analyzed animals is annotated at each figure. The statistical method used for comparison between experimental groups was a two-tailed homoscedastic Student's t test. Statistical significance was expressed as a p value.

Metabolic measurements

Blood was collected from control *Orc2*$^{f/f}$ *ROSA26*$^{stop\text{-}EYFP}$ and experimental *Alb-Orc2*$^{f/f}$ *ROSA26*$^{stop\text{-}EYFP}$ animals and centrifuged at 1000g for 10 min at 4°C. To measure Alanine Transaminase (ALT) and Aspartame Aminotransferase (AST) activities EnzyChromTM Alanine Transaminase Assay Kit (BioAssay Systems, Cat# EALT-100) and Liquid AST (SGOT) Reagent Set (Pointe Scientific, Cat# A7561150) were used respectively according to manufacturers' instructions. The number of analyzed animals is annotated at the figure. The statistical method used for comparison between experimental groups was a two-tailed homoscedastic Student's t test. Statistical significance was expressed as a p value.

Isolation of hepatocytes

Hepatocytes were isolated according to STAR protocols (Charni-Natan and Goldstein, 2020). In brief, the liver perfused with perfusion Buffer for 10 min followed by digestion buffer for 10 min was dissected out and hepatocytes were released into plating medium containing dish. A single-cell suspension was obtained by filtering through a 100-µm cell strainer. Percoll centrifugation (Cytiva #17089102) was performed to remove dead cells. Isolated live Hepatocyte were suspended in William's medium (WEM, GIBCO A1217601) with Plating Supplement (GIBCO #CM3000) and plated on collagen coated cover glass (5x10^5 cells/6-well). After 3 hrs., the medium was exchanged for maintenance medium (William's E Medium (WEM, GIBCO A1217601) supplemented with GIBCO #CM4000).

Ploidy analysis

Nuclei Isolation Medium (NIM; 250mM Sucrose, 25mM KCl, 5mM $MgCl_2$, 10mM Tris-Cl, 1mM DTT, 1x Protease inhibitor) with 2% paraformaldehyde and 0.1% Triton X-100 was added to the liver pieces that were subsequently homogenized with Pestle A Dounce homogenizer (25x times). After all samples were processed, they were centrifuged at 1000g for 10 min at 4°C. Pellet was resuspended in NIM and equal volume of 50% iodixanol was added. The mixed sample was carefully layered on the top of 29% Iodixanol solution in ultracentrifuge tube and spun at 10,300rpm for 10 minutes at 4°C in ultracentrifuge. The nuclei pellet was resuspended in FACS buffer (1x PBS, 2.5% (v/v) BSA, 2mM EDTA, 2mM NaN_3) with 100 µg/mL RNase A. DRAQ5-stained liver nuclei samples were processed using Attune NxT flow cytometer (Life Technologies). Flow cytometry data were analyzed with FCS express software. The statistical method used for

comparison between experimental groups was a two-tailed homoscedastic Student's t test. Statistical significance was expressed as a p value.

EdU incorporation in vitro

2 days after plating, Hepatocyte was labeled with 20 mM of EdU (Lumiprobe #10540) for 2 hrs and fixed with 4% paraformaldehyde for 10 min followed by permeabilized with 0.25 % Tritonx-100 for 5 min. The fixed cells were incubated with label mix [8 μM Sulfo-Cy3-Azide (Lumiprobe #B1330), 2 mM CuSO4*5H2O, 113 mM Ascorbic Acid] for 30 min. Anti-GFP antibody (Abcam #ab6556) was used to detect EYFP signal after the EdU staining.

Partial hepatectomy

The partial hepatectomy experiment was conducted following a standardized protocol (Mitchell and Willenbring, 2008). Briefly, 8-14-week-old mice were utilized. After inducing anesthesia with 2% isoflurane and maintaining at 0.2%, the mice were subcutaneously injected with Buprenorphine-SR (0.6 mg/kg) and Carprofen (5 mg/kg). The abdominal wall was shaved and prepared aseptically. A 3 cm long transverse incision was made to expose the xiphoid. The left and medium lobes were tied using 4-0 thread and cut. The incision site was double-checked for bleeding following washed with 0.9% sodium chloride and sutured. Mice were placed on a warm pad for recovery. To detect DNA synthesis, 0.2mg EDU (Lumiprobe #10540) was injected via the tail vein 3-4 hours before sacrifice. At 36-48 hours post-surgery, samples from the regenerating right liver were collected and weighed. For IHC and IF staining, samples were fixed with 4% formaldehyde, dehydrated, cleared, embedded in paraffin, and sectioned at 5-8 μm thickness. Tissue sections were deparaffinized and rehydrated, and heat antigen retrieval methods were applied in 10 mM sodium citrate buffer (pH=6.0). Permeabilization with 0.25% Triton X-100 followed EDU incorporation by Click-in reaction for 40 minutes at room temperature, protected from light. After washing and blocking, an anti-GFP antibody (Abcam, cat# ab6556, 1:500 dilution) and Alexa-488 fluorescent-conjugated secondary antibody (A11029; Life Technologies) were used to detect EYFP signaling. Finally, nuclei were stained with DAPI, and images were captured using Zeiss Confocal microscope and processed using ImageJ and GraphPad software. To improve the EYFP signal, we used frozen sections for the liver regeneration experiments in the Orc1, Orc2 double knockout mice in Fig. 6.

Bibliography

BELL, M. R. 2018. Comparing Postnatal Development of Gonadal Hormones and Associated Social Behaviors in Rats, Mice, and Humans. *Endocrinology,* 159**,** 2596-2613.

BELL, S. P. 2017. Rethinking origin licensing. *Elife,* 6.

BELL, S. P., KOBAYASHI, R. & STILLMAN, B. 1993. Yeast origin recognition complex functions in transcription silencing and DNA replication. *Science,* 262**,** 1844-9.

BELL, S. P. & STILLMAN, B. 1992. ATP-dependent recognition of eukaryotic origins of DNA replication by a multiprotein complex. *Nature,* 357**,** 128-34.

BERMEJO, R., VILABOA, N. & CALES, C. 2002. Regulation of CDC6, geminin, and CDT1 in human cells that undergo polyploidization. *Mol Biol Cell,* 13**,** 3989-4000.

BICKNELL, L. S., BONGERS, E. M., LEITCH, A., BROWN, S., SCHOOTS, J., HARLEY, M. E., AFTIMOS, S., AL-AAMA, J. Y., BOBER, M., BROWN, P. A., VAN BOKHOVEN, H., DEAN, J., EDREES, A. Y., FEINGOLD, M., FRYER, A., HOEFSLOOT, L. H., KAU, N., KNOERS, N. V., MACKENZIE, J., OPITZ, J. M., SARDA, P., ROSS, A., TEMPLE, I. K., TOUTAIN, A., WISE, C. A., WRIGHT, M. & JACKSON, A. P. 2011a. Mutations in the pre-replication complex cause Meier-Gorlin syndrome. *Nat Genet,* 43**,** 356-9.

BICKNELL, L. S., WALKER, S., KLINGSEISEN, A., STIFF, T., LEITCH, A., KERZENDORFER, C., MARTIN, C. A., YEYATI, P., AL SANNA, N., BOBER, M., JOHNSON, D., WISE, C., JACKSON, A. P., O'DRISCOLL, M. & JEGGO, P. A. 2011b. Mutations in ORC1, encoding the largest subunit of the origin recognition complex, cause microcephalic primordial dwarfism resembling Meier-Gorlin syndrome. *Nat Genet,* 43**,** 350-5.

BLEICHERT, F., BOTCHAN, M. R. & BERGER, J. M. 2015. Crystal structure of the eukaryotic origin recognition complex. *Nature,* 519**,** 321-6.

CAO, J., SPIELMANN, M., QIU, X., HUANG, X., IBRAHIM, D. M., HILL, A. J., ZHANG, F., MUNDLOS, S., CHRISTIANSEN, L., STEEMERS, F. J., TRAPNELL, C. & SHENDURE, J. 2019. The single-cell transcriptional landscape of mammalian organogenesis. *Nature,* 566**,** 496-502.

CHARNI-NATAN, M. & GOLDSTEIN, I. 2020. Protocol for Primary Mouse Hepatocyte Isolation. *STAR Protoc,* 1**,** 100086.

CHOU, H. C., BHALLA, K., DEMERDESH, O. E., KLINGBEIL, O., HANINGTON, K., AGANEZOV, S., ANDREWS, P., ALSUDANI, H., CHANG, K., VAKOC, C. R., SCHATZ, M. C., MCCOMBIE, W. R. & STILLMAN, B. 2021. The human origin recognition complex is essential for pre-RC assembly, mitosis, and maintenance of nuclear structure. *Elife,* 10.

CLAREY, M. G., ERZBERGER, J. P., GROB, P., LESCHZINER, A. E., BERGER, J. M., NOGALES, E. & BOTCHAN, M. 2006. Nucleotide-dependent conformational changes in the DnaA-like core of the origin recognition complex. *Nat Struct Mol Biol,* 13**,** 684-90.

CONFORTO, T. L. & WAXMAN, D. J. 2012. Sex-specific mouse liver gene expression: genome-wide analysis of developmental changes from pre-pubertal period to young adulthood. *Biol Sex Differ,* 3**,** 9.

COSTA, A. & DIFFLEY, J. F. X. 2022. The Initiation of Eukaryotic DNA Replication. *Annu Rev Biochem,* 91**,** 107-131.

DE RENTY, C., KANEKO, K. J. & DEPAMPHILIS, M. L. 2014. The dual roles of geminin during trophoblast proliferation and differentiation. *Dev Biol,* 387**,** 49-63.

DHAR, S. K., DELMOLINO, L. & DUTTA, A. 2001a. Architecture of the human origin recognition complex. *J Biol Chem,* 276**,** 29067-71.

DHAR, S. K., YOSHIDA, K., MACHIDA, Y., KHAIRA, P., CHAUDHURI, B., WOHLSCHLEGEL, J. A., LEFFAK, M., YATES, J. & DUTTA, A. 2001b. Replication from oriP of Epstein-Barr virus requires human ORC and is inhibited by geminin. *Cell,* 106**,** 287-96.

FOSS, M., MCNALLY, F. J., LAURENSON, P. & RINE, J. 1993. Origin recognition complex (ORC) in transcriptional silencing and DNA replication in S. cerevisiae. *Science,* 262**,** 1838-44.

GIORDANO-COLTART, J., YING, C. Y., GAUTIER, J. & HURWITZ, J. 2005. Studies of the properties of human origin recognition complex and its Walker A motif mutants. *Proc Natl Acad Sci U S A,* 102**,** 69-74.

GONZALEZ, M. A., TACHIBANA, K. E., ADAMS, D. J., VAN DER WEYDEN, L., HEMBERGER, M., COLEMAN, N., BRADLEY, A. & LASKEY, R. A. 2006. Geminin is essential to prevent endoreduplication and to form pluripotent cells during mammalian development. *Genes Dev,* 20**,** 1880-4.

GUALDI, R., BOSSARD, P., ZHENG, M., HAMADA, Y., COLEMAN, J. R. & ZARET, K. S. 1996. Hepatic specification of the gut endoderm in vitro: cell signaling and transcriptional control. *Genes Dev,* 10**,** 1670-82.

GUERNSEY, D. L., MATSUOKA, M., JIANG, H., EVANS, S., MACGILLIVRAY, C., NIGHTINGALE, M., PERRY, S., FERGUSON, M., LEBLANC, M., PAQUETTE, J., PATRY, L., RIDEOUT, A. L., THOMAS, A., ORR, A., MCMASTER, C. R., MICHAUD, J. L., DEAL, C., LANGLOIS, S., SUPERNEAU, D. W., PARKASH, S., LUDMAN, M., SKIDMORE, D. L. & SAMUELS, M. E. 2011. Mutations in origin recognition complex gene ORC4 cause Meier-Gorlin syndrome. *Nat Genet,* 43**,** 360-4.

HAYASHI, S., LEWIS, P., PEVNY, L. & MCMAHON, A. P. 2002. Efficient gene modulation in mouse epiblast using a Sox2Cre transgenic mouse strain. *Mech Dev,* 119 Suppl 1**,** S97-S101.

HU, Y. & STILLMAN, B. 2023. Origins of DNA replication in eukaryotes. *Mol Cell,* 83**,** 352-372.

JANBANDHU, V. C., MOIK, D. & FÄSSLER, R. 2014. Cre recombinase induces DNA damage and tetraploidy in the absence of loxP sites. *Cell Cycle,* 13**,** 462-70.

LILLY, M. A. & DURONIO, R. J. 2005. New insights into cell cycle control from the Drosophila endocycle. *Oncogene,* 24**,** 2765-75.

LOO, S., FOX, C. A., RINE, J., KOBAYASHI, R., STILLMAN, B. & BELL, S. 1995. The origin recognition complex in silencing, cell cycle progression, and DNA replication. *Mol Biol Cell,* 6**,** 741-56.

LOONSTRA, A., VOOIJS, M., BEVERLOO, H. B., ALLAK, B. A., VAN DRUNEN, E., KANAAR, R., BERNS, A. & JONKERS, J. 2001. Growth inhibition and DNA damage induced by Cre recombinase in mammalian cells. *Proc Natl Acad Sci U S A,* 98**,** 9209-14.

MICKLEM, G., ROWLEY, A., HARWOOD, J., NASMYTH, K. & DIFFLEY, J. F. 1993. Yeast origin recognition complex is involved in DNA replication and transcriptional silencing. *Nature,* 366**,** 87-9.

MITCHELL, C. & WILLENBRING, H. 2008. A reproducible and well-tolerated method for 2/3 partial hepatectomy in mice. *Nat Protoc,* 3**,** 1167-70.

NAICHE, L. A. & PAPAIOANNOU, V. E. 2007. Cre activity causes widespread apoptosis and lethal anemia during embryonic development. *Genesis,* 45**,** 768-75.

NEUWALD, A. F., ARAVIND, L., SPOUGE, J. L. & KOONIN, E. V. 1999. AAA+: A class of chaperone-like ATPases associated with the assembly, operation, and disassembly of protein complexes. *Genome Res,* 9**,** 27-43.

OKANO-UCHIDA, T., KENT, L. N., OUSEPH, M. M., MCCARTY, B., FRANK, J. J., KLADNEY, R., CUITINO, M. C., THOMPSON, J. C., COPPOLA, V., ASANO, M. & LEONE, G. 2018. Endoreduplication of the mouse genome in the absence of ORC1. *Genes Dev,* 32**,** 978-990.

PARK, S. Y. & ASANO, M. 2008. The origin recognition complex is dispensable for endoreplication in Drosophila. *Proc Natl Acad Sci U S A,* 105**,** 12343-8.

POSTIC, C., SHIOTA, M., NISWENDER, K. D., JETTON, T. L., CHEN, Y., MOATES, J. M., SHELTON, K. D., LINDNER, J., CHERRINGTON, A. D. & MAGNUSON, M. A. 1999. Dual roles for glucokinase in glucose homeostasis as determined by liver and pancreatic beta cell-specific gene knock-outs using Cre recombinase. *J Biol Chem,* 274**,** 305-15.

PRASANTH, S. G., PRASANTH, K. V., SIDDIQUI, K., SPECTOR, D. L. & STILLMAN, B. 2004. Human Orc2 localizes to centrosomes, centromeres and heterochromatin during chromosome inheritance. *EMBO J,* 23**,** 2651-63.

SAHA, P., CHEN, J., THOME, K. C., LAWLIS, S. J., HOU, Z. H., HENDRICKS, M., PARVIN, J. D. & DUTTA, A. 1998. Human CDC6/Cdc18 associates with Orc1 and cyclin-cdk and is selectively eliminated from the nucleus at the onset of S phase. *Mol Cell Biol,* 18**,** 2758-67.

SCHMIDT-SUPPRIAN, M. & RAJEWSKY, K. 2007. Vagaries of conditional gene targeting. *Nat Immunol,* 8**,** 665-8.

SCHMIDT, E. E., TAYLOR, D. S., PRIGGE, J. R., BARNETT, S. & CAPECCHI, M. R. 2000. Illegitimate Cre-dependent chromosome rearrangements in transgenic mouse spermatids. *Proc Natl Acad Sci U S A,* 97**,** 13702-7.

SCHNEIDER, C. A., RASBAND, W. S. & ELICEIRI, K. W. 2012. NIH Image to ImageJ: 25 years of image analysis. *Nat Methods,* 9**,** 671-5.

SEMPLE, J. W., DA-SILVA, L. F., JERVIS, E. J., AH-KEE, J., AL-ATTAR, H., KUMMER, L., HEIKKILA, J. J., PASERO, P. & DUNCKER, B. P. 2006. An essential role for Orc6 in DNA replication through maintenance of pre-replicative complexes. *EMBO J,* 25**,** 5150-8.

SHIBATA, E. & DUTTA, A. 2020. A human cancer cell line initiates DNA replication normally in the absence of ORC5 and ORC2 proteins. *J Biol Chem,* 295**,** 16949-16959.

SHIBATA, E., KIRAN, M., SHIBATA, Y., SINGH, S., KIRAN, S. & DUTTA, A. 2016. Two subunits of human ORC are dispensable for DNA replication and proliferation. *Elife,* 5.

SHU, Z., ROW, S. & DENG, W. M. 2018. Endoreplication: The Good, the Bad, and the Ugly. *Trends Cell Biol,* 28**,** 465-474.

SOHLENIUS-STERNBECK, A. K. 2006. Determination of the hepatocellularity number for human, dog, rabbit, rat and mouse livers from protein concentration measurements. *Toxicol In Vitro,* 20**,** 1582-6.

STILLMAN, B. 2022. The remarkable gymnastics of ORC. *Elife,* 11.

SU, T. T. & O'FARRELL, P. H. 1998. Chromosome association of minichromosome maintenance proteins in Drosophila endoreplication cycles. *J Cell Biol,* 140**,** 451-60.

TAKEDA, D. Y., SHIBATA, Y., PARVIN, J. D. & DUTTA, A. 2005. Recruitment of ORC or CDC6 to DNA is sufficient to create an artificial origin of replication in mammalian cells. *Genes Dev,* 19**,** 2827-36.

TILGHMAN, S. M. & BELAYEW, A. 1982. Transcriptional control of the murine albumin/alpha-fetoprotein locus during development. *Proc Natl Acad Sci U S A,* 79**,** 5254-7.

VERMEULEN, M., EBERL, H. C., MATARESE, F., MARKS, H., DENISSOV, S., BUTTER, F., LEE, K. K., OLSEN, J. V., HYMAN, A. A., STUNNENBERG, H. G. & MANN, M. 2010. Quantitative interaction proteomics and genome-wide profiling of epigenetic histone marks and their readers. *Cell,* 142**,** 967-80.

WELCH, M. 1992. Management of generalized faecal peritonitis. *J R Soc Med,* 85**,** 246.

WILLIAMS, R. S., SHOHET, R. V. & STILLMAN, B. 1997. A human protein related to yeast Cdc6p. *Proc Natl Acad Sci U S A,* 94**,** 142-7.

Table 1 Embryonic lethality of *Orc2 KO*. The *Orc2D* allele was created by expressing Cre recombinase from a *Sox2* promoter in the $Orc2^{f/+}$ embryos.

Offspring from $Orc2^{+/\Delta}$ intercrosses

stage	genotype			empty decidua	total # (litters)
	$Orc2^{+/+}$	$Orc2^{+/\Delta}$	$Orc2^{\Delta/\Delta}$		
E3.5	18	30	6	6 (n.d.)	60 (6)
E7.5	9	21	0	16	46 (5)
E13.5	9	31	0	15	55 (6)
2wk	52	115	0	-	167 (27)

Table 2 Estimate of number of hepatocyte nuclei in adult mice of indicate genotypes and thus, number of hepatocyte nuclear divisions required after E9.5 mouse embryos

	WT	*Orc2-/-*	*Orc1-/- Orc2-/- (Females)*	*Orc1-/- Orc2-/- (Males)*
Liver weight	100%	50-75%	30%	47%
Hepatocyte nuclear density	1	0.5	0.05	0.66
Total nuclei in liver (normalized to WT)	100	25-37.5	1.5	31
Deficit in # cell division	0	1-2	6-7	1-2
Number of nuclear divisions since E9.5	16-17	14-16	9-11	14-16

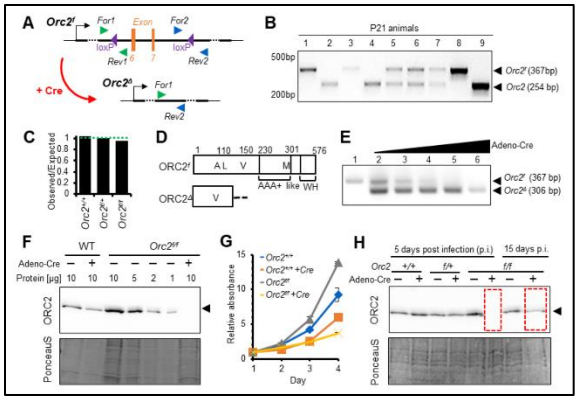

Figure 1 Generation of *Orc2*$^{f/f}$ mice and ORC2 KO MEFs.

A. Scheme of introduced loxP sites in Orc2 locus.
B. Representative picture of genotyping of offspring coming from *Orc2*$^{f/+}$ crossed with *Orc2*$^{f/+}$.
C. The ratio of observed to expected animals coming from *Orc2*$^{f/+}$ crossed with *Orc2*$^{f/+}$.
D. Schematic of the ORC2 protein and the DeltaORC2 protein produced after deletion of exons 6 and 7. A110 is mutated to V110 and then the protein goes out of frame.
E. Validation of *Orc2* deletion 3 days after Adeno cre transduction.
F. Western blot of ORC2 protein 5 days after Adeno cre transduction. 10 or indicated ul of lysate loaded/lane as written on the top
G. MTT assay of WT and *Orc2*$^{f/f}$ MEFs without and with Adeno cre transduction.
H. Western blot of ORC2 protein 5 and 15 days after Adeno cre transduction.

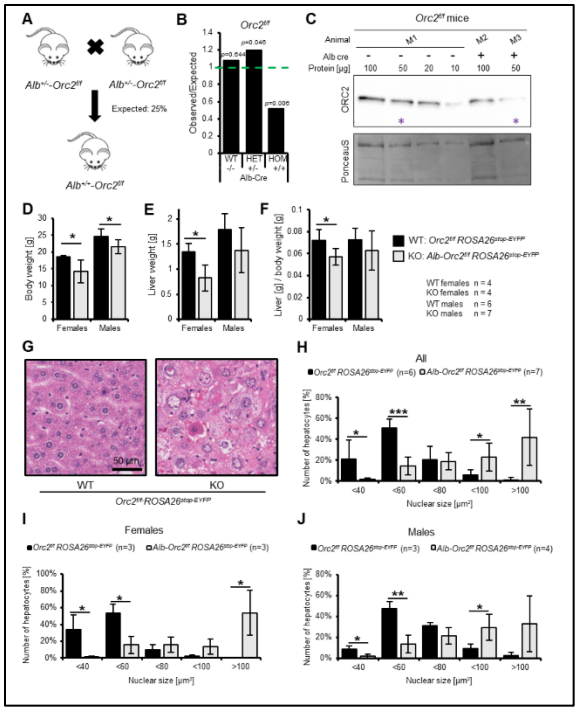

Figure 2 Development of liver in *Orc2* KO mice.

A. Scheme of Alb$^{+/-}$-*Orc2*$^{f/f}$ crossed with Alb$^{+/-}$-*Orc2*$^{f/f}$.
B. The ratio of observed to expected animals coming from A.
C. Western blot of liver tissue from *Orc2*$^{f/f}$ and *Alb-Orc2*$^{f/f}$ animals. Red stars point to lanes with comparable amounts of total loaded protein. Note that the liver has hematopoietic and other cells in addition to hepatocytes, which is why a trace amount of ORC2 will always be detected.
D. Average body weight of *Orc2*$^{f/f}$ *ROSA26*$^{stop\text{-}EYFP}$ and *Alb-Orc2*$^{f/f}$ *ROSA26*$^{stop\text{-}EYFP}$ animals.
E. Average liver weight of *Orc2*$^{f/f}$ *ROSA26*$^{stop\text{-}EYFP}$ and *Alb-Orc2*$^{f/f}$ *ROSA26*$^{stop\text{-}EYFP}$ animals.
F. Average liver to body weight ratio of *Orc2*$^{f/f}$ *ROSA26*$^{stop\text{-}EYFP}$ and *Alb-Orc2*$^{f/f}$ *ROSA26*$^{stop\text{-}EYFP}$ animals.
G. Representative H&E staining of liver tissue from *Orc2*$^{f/f}$ *ROSA26*$^{stop\text{-}EYFP}$ (WT) and *Alb-Orc2*$^{f/f}$ *ROSA26*$^{stop\text{-}EYFP}$ (KO) animals.
H. Quantification of hepatocyte nuclear size in *Orc2*$^{f/f}$ *ROSA26*$^{stop\text{-}EYFP}$ and *Alb-Orc2*$^{f/f}$ *ROSA26*$^{stop\text{-}EYFP}$ animals.
I. Quantification of hepatocyte nuclear size in *Orc2*$^{f/f}$ *ROSA26*$^{stop\text{-}EYFP}$ and *Alb-Orc2*$^{f/f}$ *ROSA26*$^{stop\text{-}EYFP}$ female mice.
J. Quantification of hepatocytes nuclear size in *Orc2*$^{f/f}$ *ROSA26*$^{stop\text{-}EYFP}$ and *Alb-Orc2*$^{f/f}$ *ROSA26*$^{stop\text{-}EYFP}$ male mice.
*$p < 0.05$, **$p < 0.01$, two-tailed Student's t test.

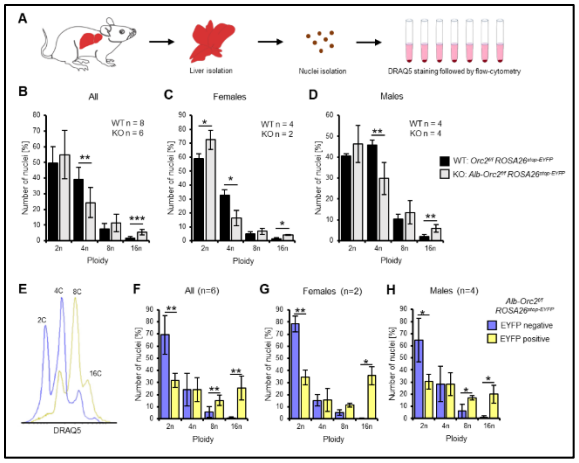

Figure 3 Endoreduplication in the *Orc2* liver conditional knock-out animals.

A. Experimental design.
B-D. Quantification of nuclei ploidy in the livers of *Orc2*$^{f/f}$ *ROSA26*$^{stop\text{-}EYFP}$ and *Alb-Orc2*$^{f/f}$ *ROSA26*$^{stop\text{-}EYFP}$ animals.
E. Representative result of flow cytometry analysis for *Alb-Orc2*$^{f/f}$ *ROSA26*$^{stop\text{-}EYFP}$ animals. The light blue and yellow profiles are from the EYFP negative and positive cells, respectively.
F-H. Quantification of nuclei ploidy for EYFP low (negative) and high (positive) primary hepatocytes.
*$p < 0.05$, **$p < 0.01$, ***$p < 0.001$, two-tailed Student's t test.

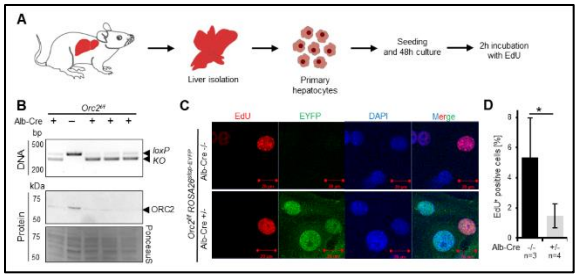

Figure 4 *Orc2* KO primary hepatocytes can incorporate EdU *in vitro*.

A. Experimental design
B. Genotyping and western blotting of hepatocytes
C. Representative picture of EdU, EYFP and DAPI staining on the *Orc2* WT and KO primary hepatocytes.
D. The percentage of EdU positive nuclei from *Orc2* WT or *Orc2* KO primary hepatocytes.
*$p < 0.05$, two-tailed Student's t test.

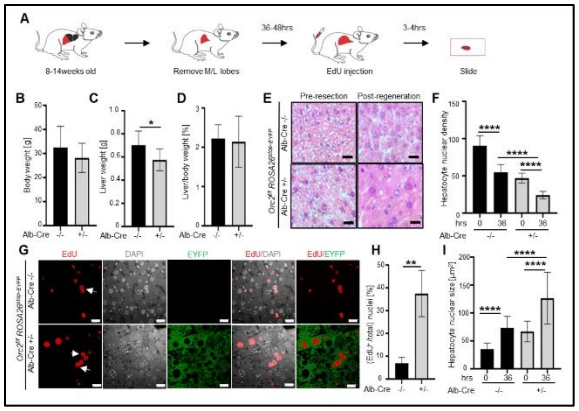

Figure 5 The ORC2 mutant livers regenerate after partial hepatectomy.

A. Schematic of the experiment.
B. Body weight of the *Orc2$^{f/f}$ ROSA26stop-EYFP* mice without (-/-) or with *Alb-Cre* (-/+) before partial hepatectomy.
C. Liver weight of the mice in B after liver regeneration.
D. Regenerated Liver to pre-hepatectomy body weight ratio of the mice in B.
E. H&E stain of *Orc2$^{f/f}$ ROSA26stop-EYFP* livers with intact *Orc2* (*Alb-cre -/-*, N=3) or *Orc2* knockout (*Alb-cre+/-*, N=7). Scale bar: 25 µm.
F. Quantitation of nuclear counts per field (76,000 um2). Six images were taken for each liver. 0 hr (pre-resection). 36 hr (post-regeneration).
G. EdU incorporation of indicated livers. EYFP marks cells where Cre has been expressed. Scale bar: 25µm.
H. Percent EdU+ nuclei counted in 1882 and 825 nuclei in the *Cre-* and *Cre+* livers, respectively.
I. Nuclear size of indicated livers. 0 hr (pre-resection). 36 hr (post-regeneration). Mean and S.D from about 40-70 nuclei, *$p < 0.05$, ****$p < 0.0001$, unpaired two-tailed Student's t test is used

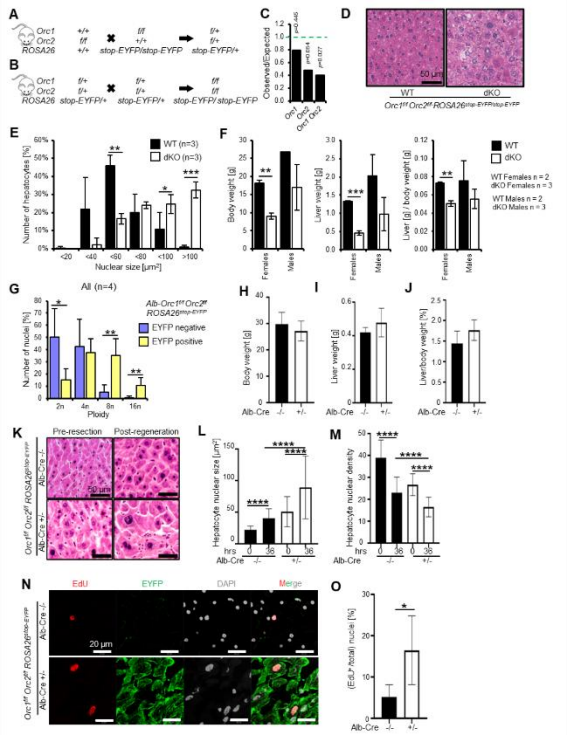

Figure 6 Endoreduplication in liver of *Orc1 Orc2 KO* animals.

A-B. Breeding schemes to obtain conditional double flox animals.
C. The ratio of observed to expected animals coming from B. *Orc1* = all animals with *Orc1$^{f/f}$ ROSA26stop-EYFP*, *Orc2* = all animals with *Orc2f/f ROSA26stop-EYFP*, *Orc1 Orc2* = all animals with *Orc1$^{f/f}$ Orc2$^{f/f}$ ROSA26stop-EYFP* genotype. This was before introduction of *Alb-Cre*.
D. Representative H&E staining of liver tissue from male *Orc1$^{f/f}$ Orc2$^{f/f}$ ROSA26stop-EYFP* (WT) and *Alb-Cre*, *Orc1$^{f/f}$ Orc2$^{f/f}$ ROSA26stop-EYFP* (dKO) animals.
E. Quantification of hepatocyte nuclear size in the WT and DKO animals.
F. Average body, liver weight and their ratio for WT and DKO animals.
G. Quantification of nuclei ploidy for EYFP low (negative) and high (positive) primary hepatocytes.
H-J. Body weight pre-resection, liver weight post-regeneration and regenerated liver to body weight ratio in mice with indicated genotypes. 4 males of *Orc1f/f Orc2f/f ROSA26stop-EYFP* mice with *Alb-Cre* (-/-) were used as control group and 6 males of *Orc1f/f Orc2f/f ROSA26stop-EYFP* mice with *Alb-Cre* (+/-) were used as experimental group. No significant difference between the two groups using two tailed Student t-test.
K: H&E stain of *Orc1$^{f/f}$ Orc2$^{f/f}$ ROSA26stop-EYFP* mice livers with intact *Orc1, Orc2* (*Alb-cre -/-*, N=4) or *Orc1,Orc2 DKO* (*Alb-cre +/-*, N=6). Scale bar: 50 µm.
L. Quantitation of hepatocyte nuclear size post regeneration. 0 hr (pre-resection). 36 hr (post-regeneration). Five-six images were taken for each liver. About 120-200 nuclei are counted.
M: Quantitation of hepatocyte nuclear density post regeneration. 0 hr (pre-resection). 36 hr (post-regeneration). Five-six images were taken for each liver.
N. Micrographs of EdU, DAPI and EYFP imaging of livers with indicated genotypes post regeneration.
Scale bar: 20 µm.

O. Quantitation of EdU positive nuclei post regeneration. Five-six images were taken for each liver.

*$p < 0.05$, ****$p < 0.0001$, unpaired two-tailed Student's t test were used

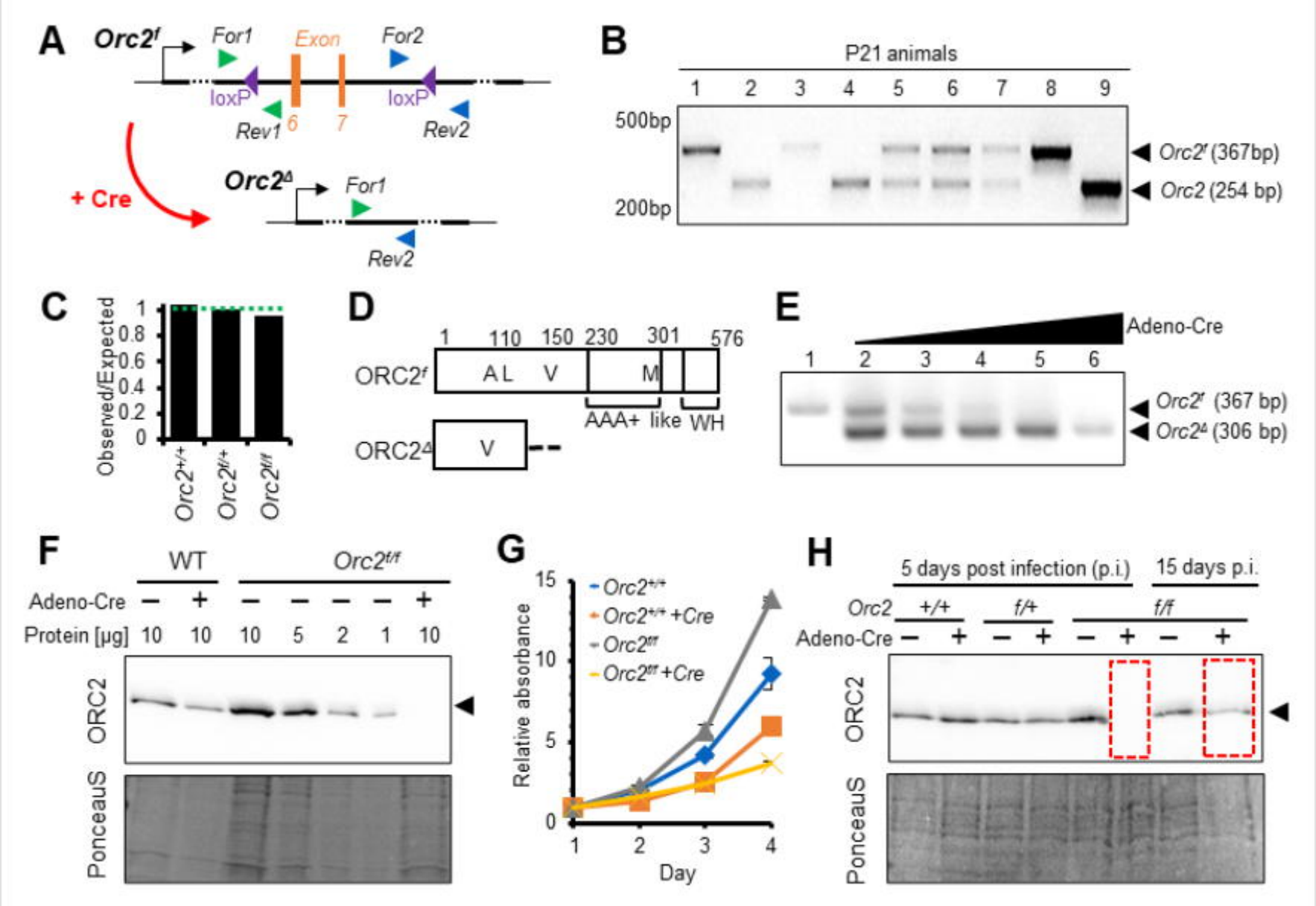
A
Orc2f
For1
Exon
For2
loxP
loxP
Rev1
6
7
Rev2
+ Cre
Orc2Δ
For1
Rev2
B
P21 animals
1 2 3 4 5 6 7 8 9
500bp
200bp
Orc2f (367bp)
Orc2 (254 bp)
C
Observed/Expected
1
0.8
0.6
0.4
0.2
0
Orc2+/+
Orc2f/+
Orc2f/f
D
1 110 150 230 301 576
ORC2f
AL V M
AAA+ like WH
ORC2Δ
V
E
Adeno-Cre
1 2 3 4 5 6
Orc2f (367 bp)
Orc2Δ (306 bp)
F
WT
Orc2f/f
Adeno-Cre – + – – – – +
Protein [µg] 10 10 10 5 2 1 10
ORC2
PonceauS
G
Orc2+/+
Orc2+/+ +Cre
Orc2f/f
Orc2f/f +Cre
Relative absorbance
15
10
5
0
1 2 3 4
Day
H
5 days post infection (p.i.)
15 days p.i.
Orc2 +/+ f/+ f/f
Adeno-Cre – + – + – + – +
ORC2
PonceauS

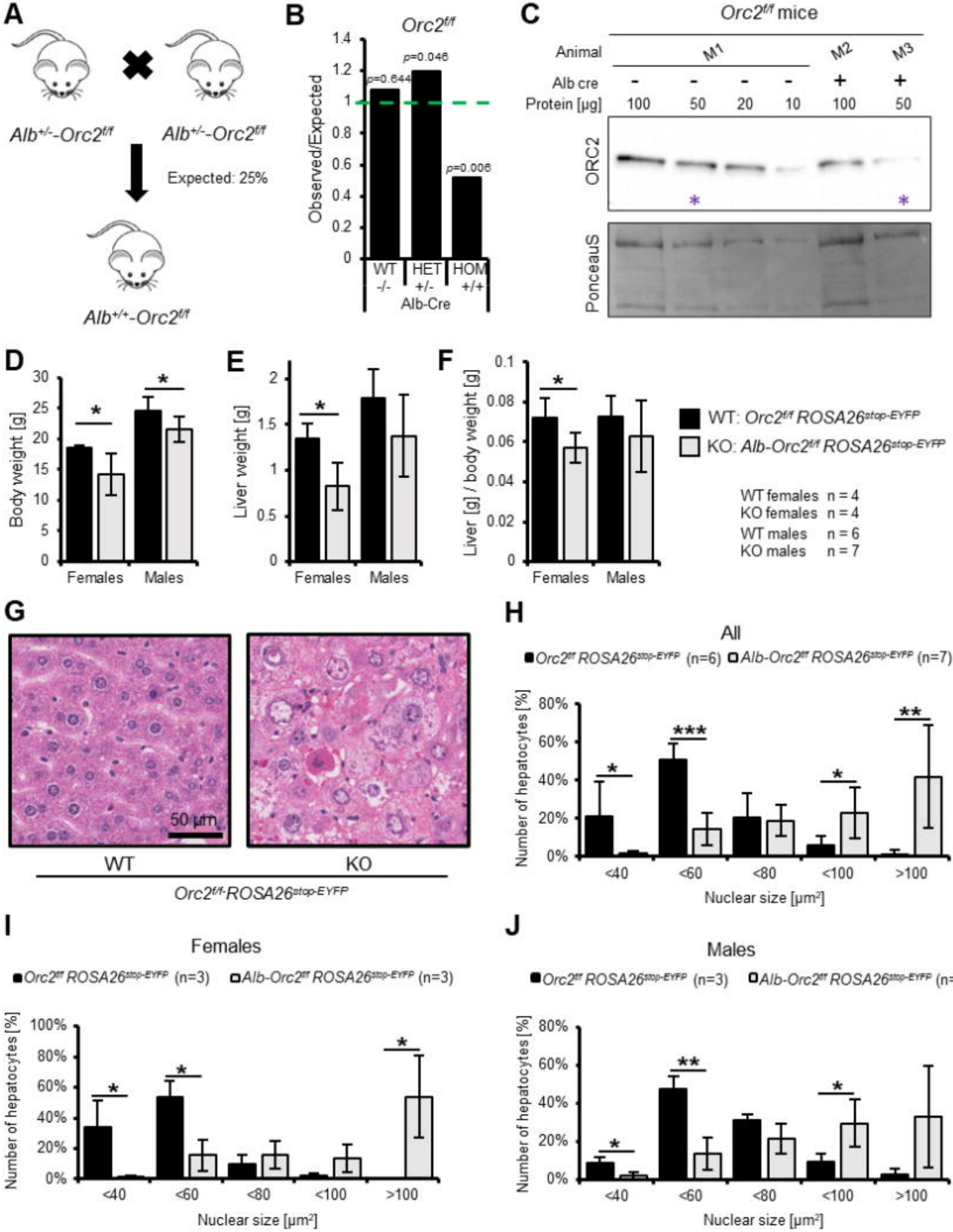
A
Alb+/--Orc2f/f
Alb+/--Orc2f/f
Expected: 25%
Alb+/+-Orc2f/f
B
Orc2f/f
Observed/Expected
p=0.644
p=0.046
p=0.006
WT -/-
HET +/-
HOM +/+
Alb-Cre
C
Orc2f/f mice
Animal
M1
M2
M3
Alb cre
Protein [µg]
ORC2
PonceauS
D
Body weight [g]
Females
Males
E
Liver weight [g]
F
Liver [g] / body weight [g]
WT: Orc2f/f ROSA26stop-EYFP
KO: Alb-Orc2f/f ROSA26stop-EYFP
WT females n = 4
KO females n = 4
WT males n = 6
KO males n = 7
G
50 µm
WT
KO
Orc2f/f-ROSA26stop-EYFP
H
All
Orc2f/f ROSA26stop-EYFP (n=6)
Alb-Orc2f/f ROSA26stop-EYFP (n=7)
Number of hepatocytes [%]
Nuclear size [µm²]
I
Females
Orc2f/f ROSA26stop-EYFP (n=3)
Alb-Orc2f/f ROSA26stop-EYFP (n=3)
J
Males
Orc2f/f ROSA26stop-EYFP (n=3)
Alb-Orc2f/f ROSA26stop-EYFP (n=4)

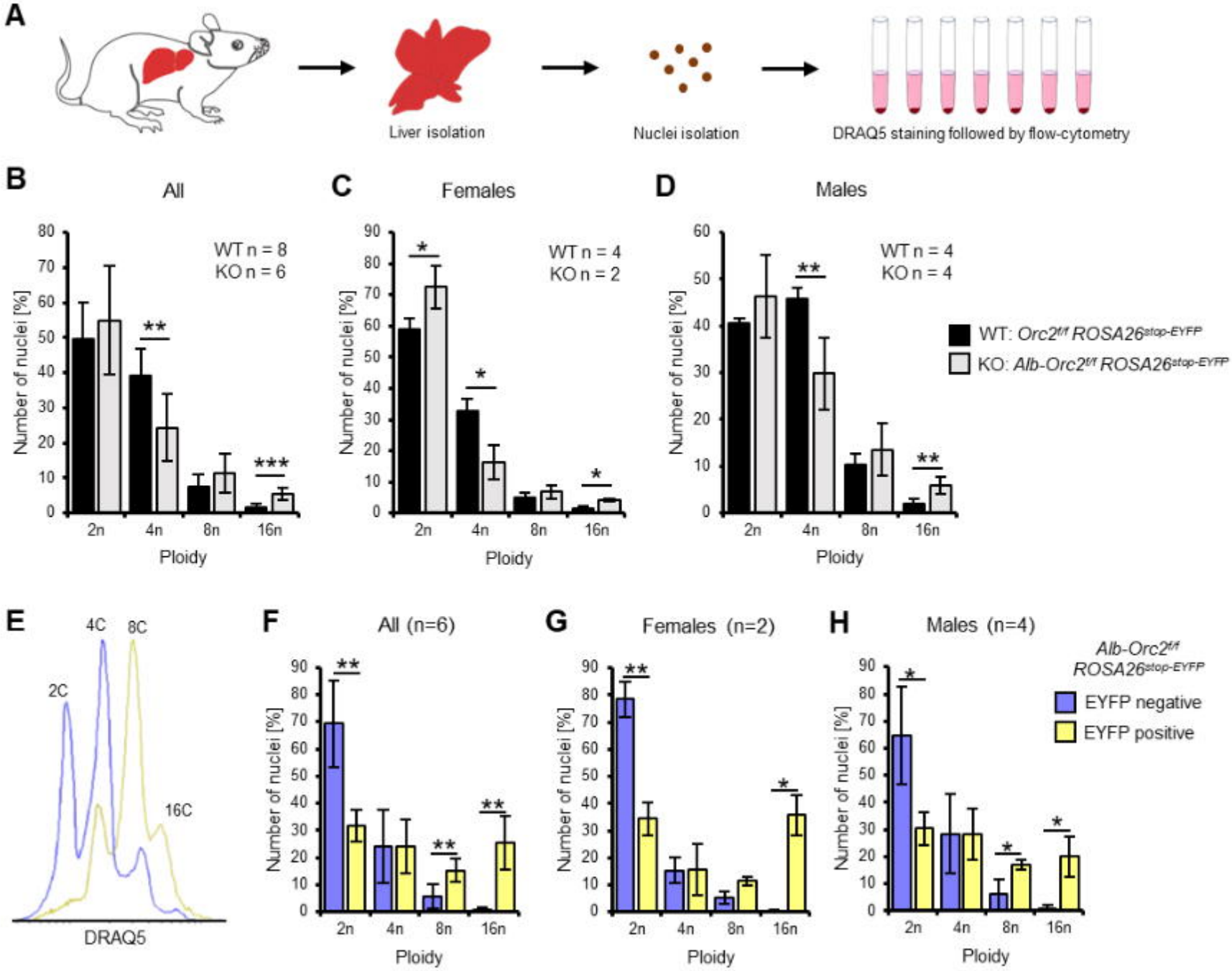
A
Liver isolation
Nuclei isolation
DRAQ5 staining followed by flow-cytometry
B
All
WT n = 8
KO n = 6
Number of nuclei [%]
Ploidy
2n
4n
8n
16n
C
Females
WT n = 4
KO n = 2
D
Males
WT n = 4
KO n = 4
WT: Orc2f/f ROSA26stop-EYFP
KO: Alb-Orc2f/f ROSA26stop-EYFP
E
2C
4C
8C
16C
DRAQ5
F
All (n=6)
G
Females (n=2)
H
Males (n=4)
Alb-Orc2f/f
ROSA26stop-EYFP
EYFP negative
EYFP positive

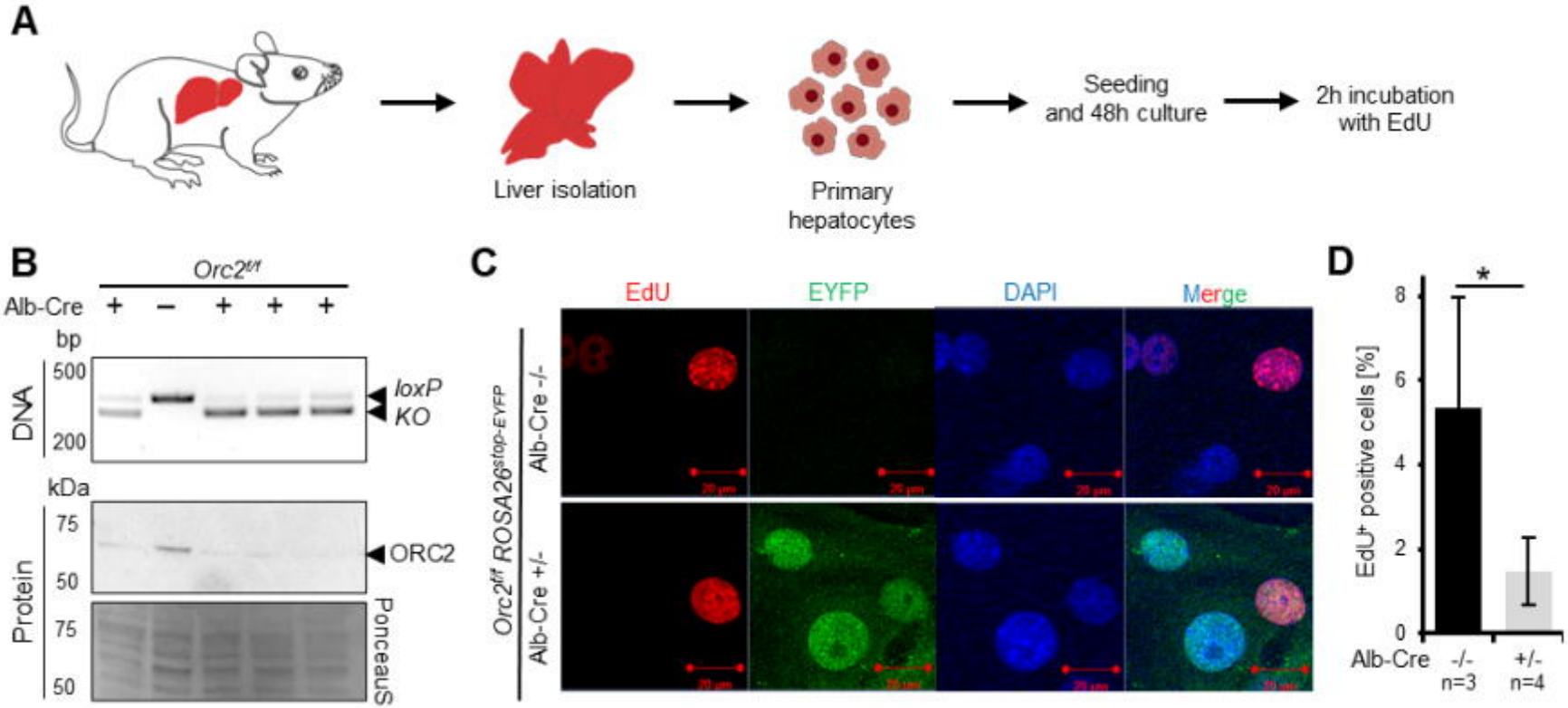
A
Liver isolation
Primary hepatocytes
Seeding and 48h culture
2h incubation with EdU
B
Orc2f/f
Alb-Cre + − + + +
bp
500
200
DNA
loxP
KO
kDa
75
50
Protein
ORC2
75
50
PonceauS
C
EdU
EYFP
DAPI
Merge
Orc2f/f ROSA26stop-EYFP
Alb-Cre -/-
Alb-Cre +/-
D
*
EdU+ positive cells [%]
8
6
4
2
0
Alb-Cre -/- +/-
n=3 n=4

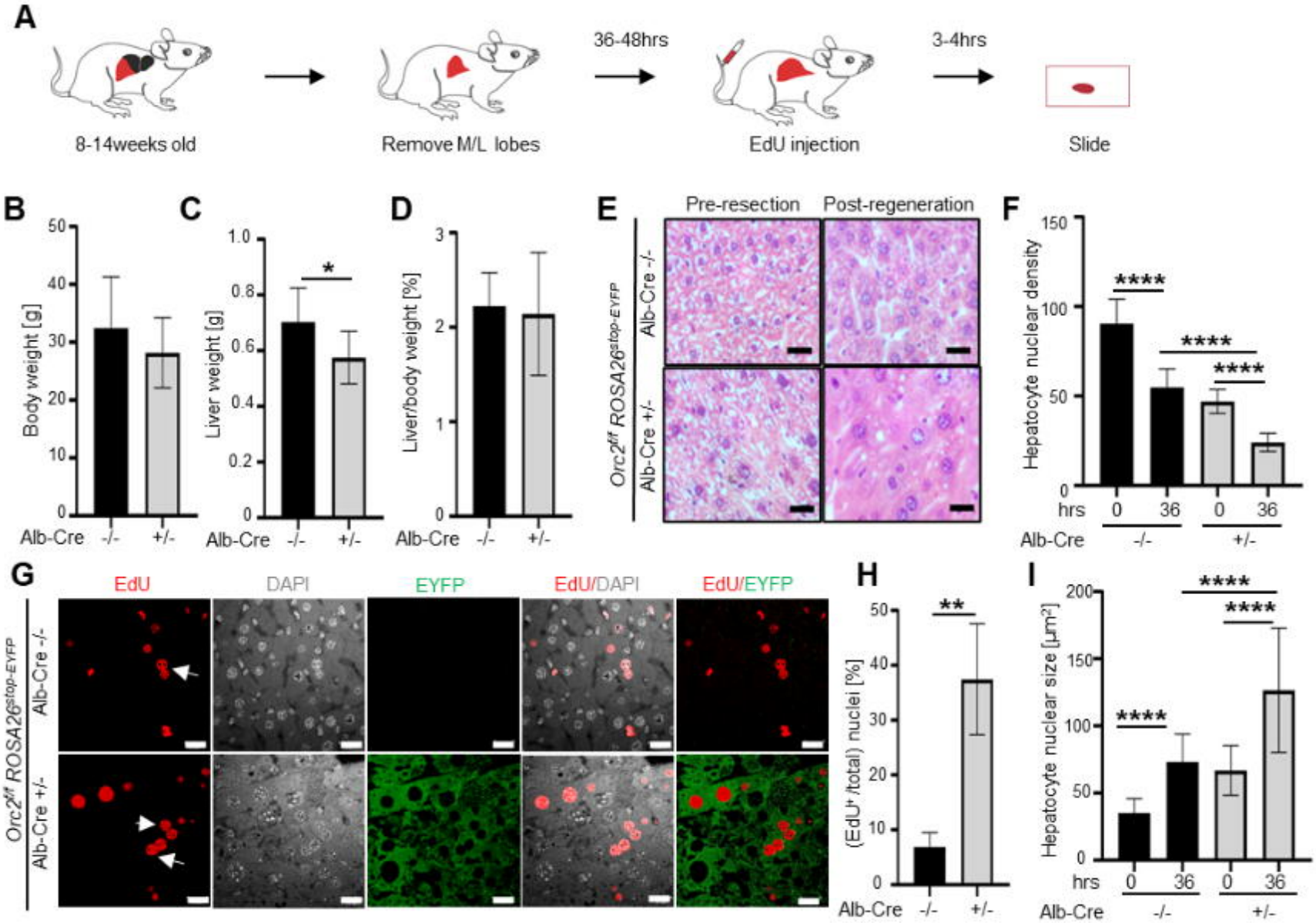
A
8-14weeks old
Remove M/L lobes
36-48hrs
EdU injection
3-4hrs
Slide
B
Body weight [g]
Alb-Cre -/- +/-
C
Liver weight [g]
*
Alb-Cre -/- +/-
D
Liver/body weight [%]
Alb-Cre -/- +/-
E
Pre-resection
Post-regeneration
Orc2f/f ROSA26stop-EYFP
Alb-Cre -/-
Alb-Cre +/-
F
Hepatocyte nuclear density
****
****
****
hrs 0 36 0 36
Alb-Cre -/- +/-
G
EdU
DAPI
EYFP
EdU/DAPI
EdU/EYFP
Orc2f/f ROSA26stop-EYFP
Alb-Cre -/-
Alb-Cre +/-
H
(EdU+ /total) nuclei [%]
**
Alb-Cre -/- +/-
I
Hepatocyte nuclear size [µm²]
****
****
****
hrs 0 36 0 36
Alb-Cre -/- +/-

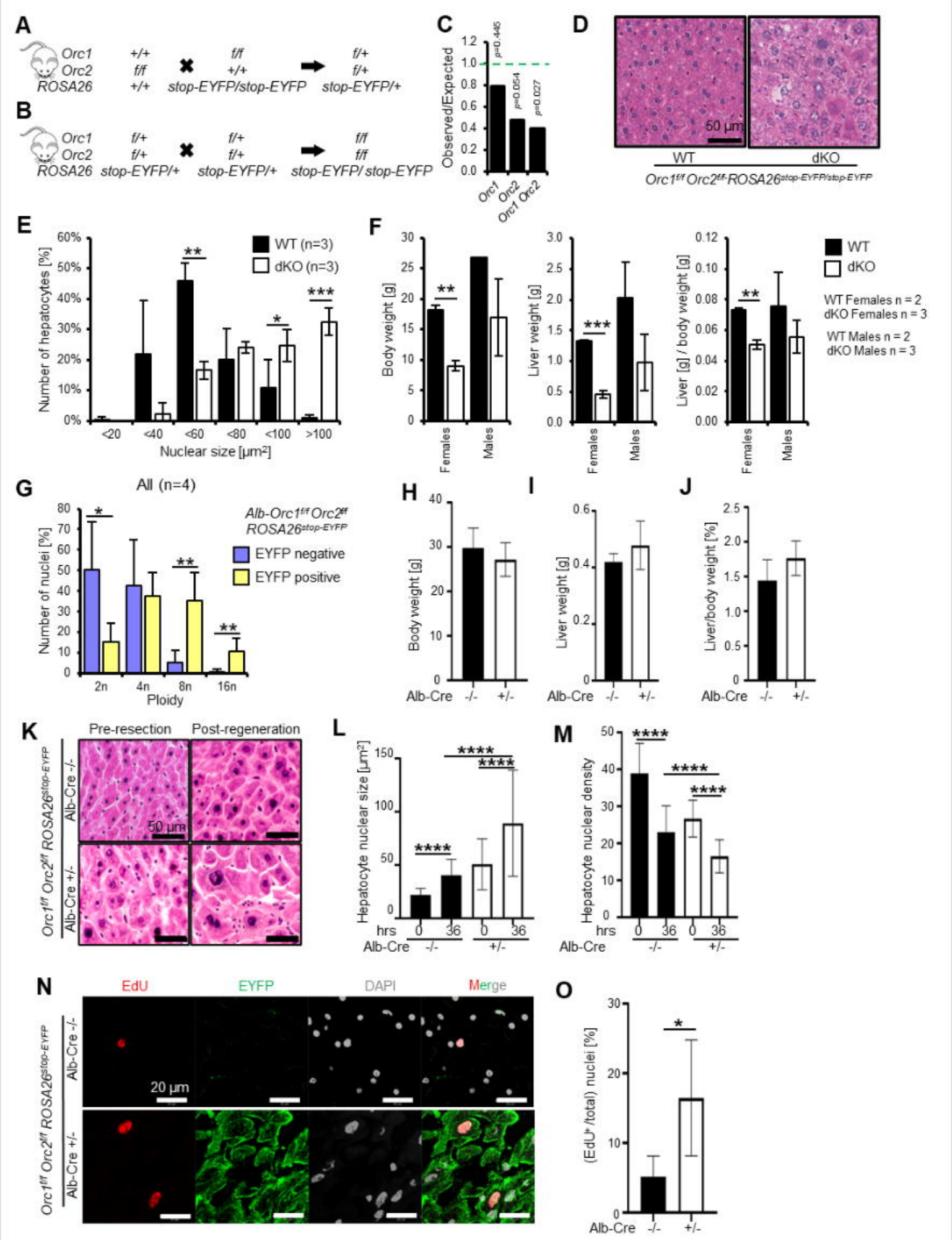
A
Orc1 +/+ f/f f/+
Orc2 f/f +/+ f/+
ROSA26 +/+ stop-EYFP/stop-EYFP stop-EYFP/+
B
Orc1 f/+ f/+ f/f
Orc2 f/+ f/+ f/f
ROSA26 stop-EYFP/+ stop-EYFP/+ stop-EYFP/ stop-EYFP
C
Observed/Expected
p=0.445
p=0.054
p=0.027
Orc1
Orc2
Orc1 Orc2
D
50 µm
WT
dKO
Orc1f/f Orc2f/f ROSA26stop-EYFP/stop-EYFP
E
Number of hepatocytes [%]
WT (n=3)
dKO (n=3)
Nuclear size [µm²]
F
Body weight [g]
Liver weight [g]
Liver [g] / body weight [g]
Females
Males
WT
dKO
WT Females n = 2
dKO Females n = 3
WT Males n = 2
dKO Males n = 3
G
All (n=4)
Number of nuclei [%]
Alb-Orc1f/f Orc2f/f ROSA26stop-EYFP
EYFP negative
EYFP positive
Ploidy
H
Body weight [g]
I
Liver weight [g]
J
Liver/body weight [%]
Alb-Cre -/- +/-
K
Pre-resection
Post-regeneration
Alb-Cre -/-
Alb-Cre +/-
Orc1f/f Orc2f/f ROSA26stop-EYFP
50 µm
L
Hepatocyte nuclear size [µm²]
hrs 0 36 0 36
Alb-Cre -/- +/-
M
Hepatocyte nuclear density
N
EdU
EYFP
DAPI
Merge
20 µm
O
(EdU+/total) nuclei [%]

Offspring from *Orc2*$^{+/\Delta}$ intercrosses

stage	genotype			empty decidua	total # (litters)
	Orc2$^{+/+}$	*Orc2*$^{+/\Delta}$	*Orc2*$^{\Delta/\Delta}$		
E3.5	18	30	6	6 (n.d.)	60 (6)
E7.5	9	21	0	16	46 (5)
E13.5	9	31	0	15	55 (6)
2wk	52	115	0	-	167 (27)

	WT	*Orc2-/-*	*Orc1-/- Orc2-/- (Females)*	*Orc1-/- Orc2-/- (Males)*
Liver weight	100%	50-75%	30%	47%
Hepatocyte nuclear density	1	0.5	0.05	0.66
Total nuclei in liver (normalized to WT)	100	25-37.5	1.5	31
Deficit in # cell division	0	1-2	6-7	1-2
Number of nuclear divisions since E9.5	16-17	14-16	9-11	14-16